

Supplementary Materials

CFTR-rich ionocytes mediate chloride absorption across airway epithelia

Lei Lei¹, Soumba Traore¹, Guillermo S. Romano Ibarra², Philip H. Karp^{2,3},
Tayyab Rehman^{2†}, David K. Meyerholz⁴, Joseph Zabner², David A. Stoltz^{2,5,6},
Patrick L. Sinn^{1,7}, Michael J. Welsh^{2,3,6}, Paul B. McCray Jr.^{1,7*} and Ian M. Thornell^{2*}

¹Stead Family Department of Pediatrics and Pappajohn Biomedical Institute Roy J. and Lucille A. Carver College of Medicine, University of Iowa, Iowa City, IA 52242, USA;

²Department of Internal Medicine and Pappajohn Biomedical Institute Roy J. and Lucille A. Carver College of Medicine, University of Iowa, Iowa City, USA;

³Howard Hughes Medical Institute, University of Iowa, Iowa City, USA;

⁴Department of Pathology, Roy J. and Lucille A. Carver College of Medicine, University of Iowa, Iowa City, USA;

⁵Department of Biomedical Engineering, University of Iowa, Iowa City, USA;

⁶Department of Molecular Physiology and Biophysics, Roy J. and Lucille A. Carver College of Medicine, University of Iowa, Iowa City, USA;

⁷Department of Microbiology and Immunology, Roy J. and Lucille A. Carver College of Medicine, University of Iowa, Iowa City, USA.

†Present address: Department of Internal Medicine, University of Michigan, Ann Arbor, USA

*These authors contributed equally to this work.

Address correspondence to:

Ian M. Thornell
169 Newton Road
6332 PBDB
Iowa City, IA 52242 USA
Phone: (319) 335-7574
Email: ian-thornell@uiowa.edu

Paul B. McCray Jr.
169 Newton Road
6320 PBDB
Iowa City, IA 52242 USA
Phone: (319) 356-1828
Email: paul-mccray@uiowa.edu

Conflict of Interest Statement: The authors have declared that no conflict of interest exists.

Supplemental Table 1

Target	Fold-change from control	<i>P</i> value
<i>FOXI1</i>	441.5 ± 101.4	0.0032
<i>CFTR</i>	7.7 ± 1.7	0.0045
<i>BSND</i>	116.7 ± 30.3	0.0047
<i>CLCNKA</i>	1.3 ± 0.6	0.3937
<i>CLCNKB</i>	20.4 ± 5.4	0.0056
<i>NGFR</i>	2.9 ± 1.2	0.0551
<i>ASCL3</i>	43.4 ± 12.5	0.0065
<i>RARRES2</i>	5.5 ± 3.4	0.0763
<i>ATP6V0D2</i>	244.0 ± 38.2	0.0010
<i>ATP6V0B</i>	2.8 ± 2.0	0.1824
<i>ATP6V1B1</i>	4.0 ± 2.0	0.0554
<i>TMPRSS11E</i>	44.9 ± 11.3	0.0044
<i>CD24</i>	2.1 ± 0.3	0.0069
<i>PPARG</i>	1.9 ± 0.6	0.0570
<i>FOXI2</i>	4.0 ± 1.3	0.1012

1 **Supplemental Table 1 RT-qPCR of ionocyte transcripts for FOXI1-OE vs. control**
2 **epithelia.** Each FOXI1-OE sample represents the fold-change from its donor-matched control
3 epithelia. *n* = 4 human donors. Error represents standard deviation of the mean. *P* values were
4 obtained using the one-sample *t* test with a hypothetical fold-change of 1.
5

Supplemental Table 2

Guide				
Target	Exon	Guide 1	Guide 2	Deletion Length
<i>FOXII</i>	1	CATAGTAGAGGTTTCATCTCGGGG	ACAACAAGAGCAAGGCCGGCTGG	412 base pairs
<i>BSND</i>	1	CCAGCACAATGAAGCCGATCCGG	TAGAAGGTGCCGTAGACCTGGGG	70 base pairs
PCR Primers				
Target		Forward	Reverse	Ref ID
<i>FOXII</i>		5'-TCTAGCATGTCATTAGTGGGGACCT	5'-TGGAGATGCAGATGAATCGTAAT	NM_012188.5
<i>BSND</i>		5'-TCTCTCCCTGTGTAAGCCTGT	5'-GGGGTCAGCGCTCATTAGCT	NM_057176.3

- 1 **Supplemental Table 2 Guide RNA and qPCR primers used to evaluate efficiency.** The upper
- 2 portion of the table lists our guide sequences used to disrupt target genes and their predicted base
- 3 pair deletion length. The lower portion of the table lists our primers pairs used for genomic
- 4 PCRs.

Supplemental Table 3

Target	Guide	Benchling Scores		inDelphi Scores	
		On Target	Off Target	Precision Score (Percentile)	Frameshift Frequency (Percentile)
<i>FOXII</i>	1	60.9	86.4	93.9	84.3
	2	55.7	68.9	97.8	88.8
<i>BSND</i>	1	48.2	84.0	98.4	75.1
	2	65.9	79.5	79.3	85.3

1 **Supplemental Table 3 Scores for guide RNAs used in this study.** The table lists scores for
2 guide sequences first obtained using Benchling then verified using inDelphi. References for the
3 Benchling and inDelphi algorithms are provided within Methods.

4

Supplemental Table 4

Target	Forward	Reverse	Ref ID
<i>RARRES2</i>	5'-GAGGGACTGGAAGAAACCCGA	5'-CTGTCCAGGGAAGTAGAAGCTGT	NM_002889.4
<i>ASCL3</i>	5'-GGACAACAGAGGCAACTCTAGT	5'-AGGGGCAGGGTTCAGTGAAT	NM_020646.3
<i>ATP6V0D2</i>	5'-TCTGATCGAAACGCCATTAGC	5'-CTTCTTTGCTCAATTCAGTGCC	NM_152565.1
<i>ATP6V0B</i>	5'-CCATCGGAACTACCATGCAGG	5'-TCCACAGAAGAGGTTAGACAGG	NM_004047.5
<i>ATP6V1B1</i>	5'-CAAGGCGATTGTTCAGGTGTT	5'-TCCCCTGTAAATTCGCAAGTG	NM_001692.4
<i>FOXI1</i>	5'-GAACTCCATCCGCCACAACC	5'-GGCTGTGCTAGAGGAAACATCT	NM_012188.5
<i>CLCNKB</i>	5'-GTGGGCATAGTGCGAAGGG	5'-CAAAGAGGTTGTGTGCCTCAT	NM_001165945.2
<i>TMPRSS11E</i>	5'-CAGTGGGATGGGAGTCATCG	5'-CTGGCAGGGTTCTTATATGTTGT	NM_014058.4
<i>CFTR</i>	5'-AGTGGAGGAAAGCCTTTGGAGT	5'-ACAGATCTGAGCCCAACCTCA	NM_000492.4
<i>CLCNKA</i>	5'-ACCCTGACGCTATTCTCAGAG	5'-CGATGTCACGAAGAGGGACTG	NM_004070.4
<i>BSND</i>	5'-GGAAAGACGCCTAACTCAGAGC	5'-CCTCCCTGTCATGTGGAGATG	NM_057176.3
<i>TMEM61</i>	5'-CACCCACGGAGTATCCGGT	5'-CACAGTGAGGTTAGTACAGGTCT	NM_182532.3
<i>CD24</i>	5'-CTCCTACCCACGCAGATTTATTC	5'-AGAGTGAGACCACGAAGAGAC	NM_013230.3
<i>NGFR</i>	5'-CCGTTGGATTACACGGTCCAC	5'-TGAAGGCTATGTAGGCCACAA	NM_002507.4
<i>PPARG</i>	5'-ACCAAAGTGCAATCAAAGTGGA	5'-ATGAGGGAGTTGGAAGGCTCT	NM_001354668.2
<i>FOXI2</i>	5'-CTGGCGGGCGACTTTTCTT	5'-GGGAGGGGTTAAGGGTCTG	NM_207426.3

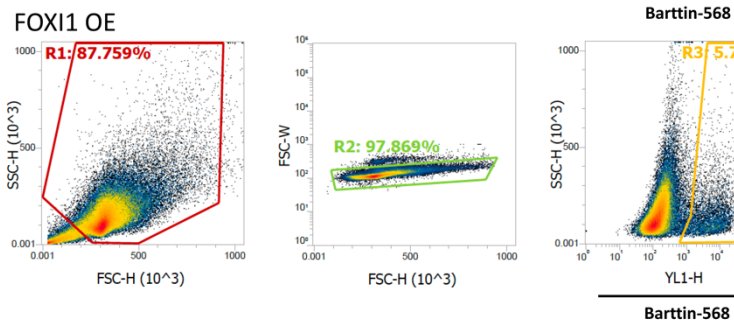
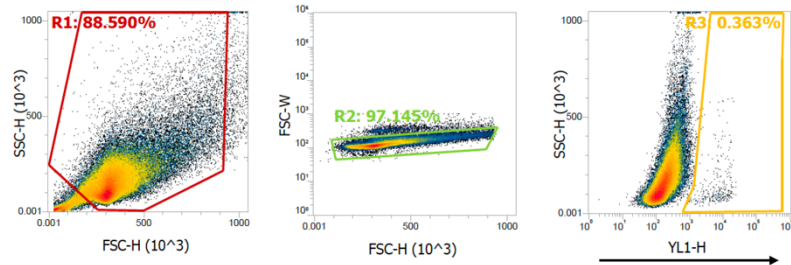
1 **Supplemental Table 4 RT-qPCR primers used in this study.**

2

Supplemental Figure 1

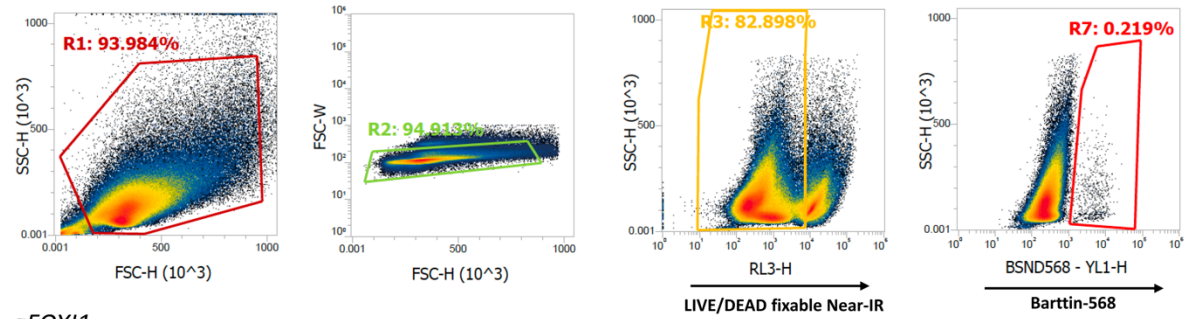
A Figure 1A Example Plots

Control

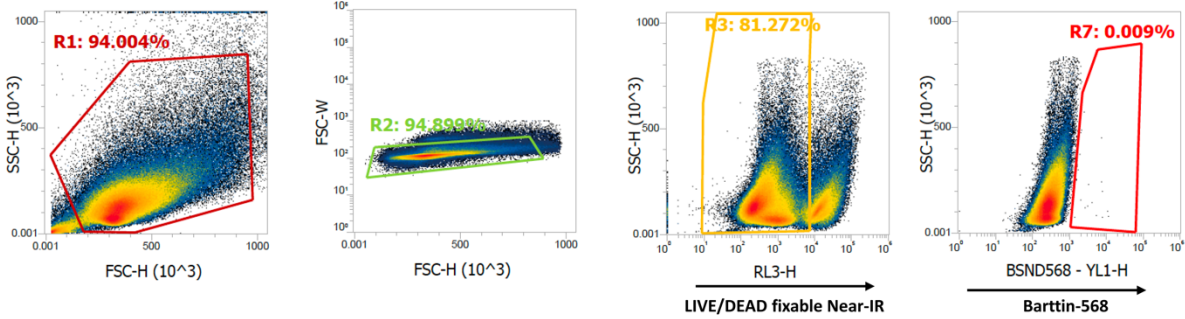


B Figure 1B Example Plots

Control

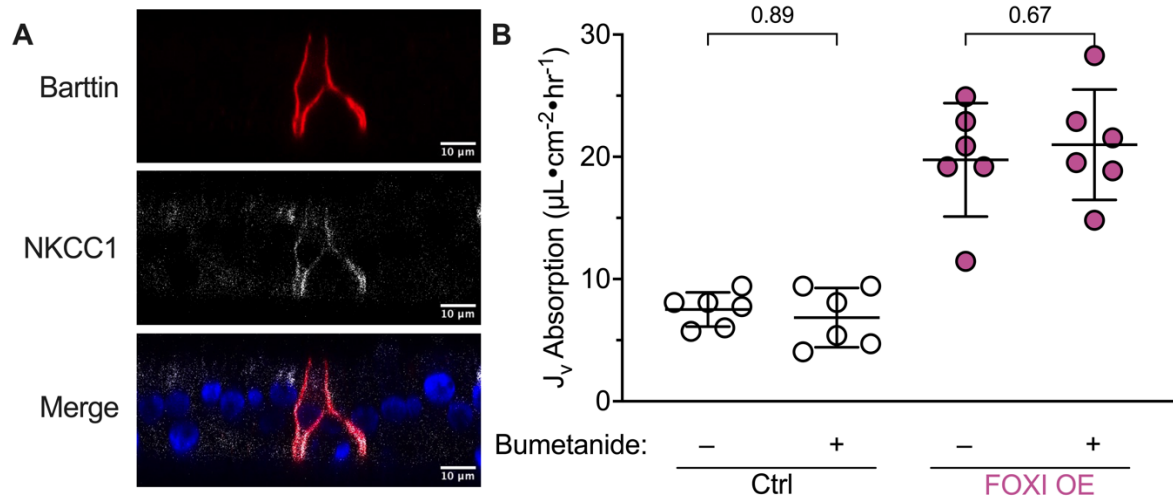


gFOXI1



1 **Supplemental Figure 1 Example flow cytometry analysis for Figure 1, A and B.** Epithelia
2 were transduced with a lentiviral vector expressing either GFP or a bicistronic construct
3 expressing FOXI1 and GFP to generate and label ionocytes (FOXI1-OE), or they were
4 electroporated with CRISPR/Cas9 and guide RNAs (gRNA) targeting *FOXII* (*gFOXII*) to
5 decrease ionocyte abundance. Cells were gated by light intensities detected by a flow cytometer.
6 **(A)** Example **Figure 1A**-type experiments with FOXI-OE epithelia and controls. The gating
7 scheme is shown from left to right. Side scatter height (SSC-H) vs. forward scatter height (FSC-
8 H) was used to select for large and granular cells. FSC-width (FSC-W) vs. FSC-H was used to
9 exclude cellular debris and clumping. Barttin was detected within the selected population. **(B)**
10 Example **Figure 1B**-type experiments for *gFOXII* epithelia and controls. The first 2 gates are as
11 described for Panel A. Then, cells were gated for intact plasma membranes, then barttin. CF
12 epithelia (**Figure 2, A and B**) underwent identical gating.

Supplemental Figure 2

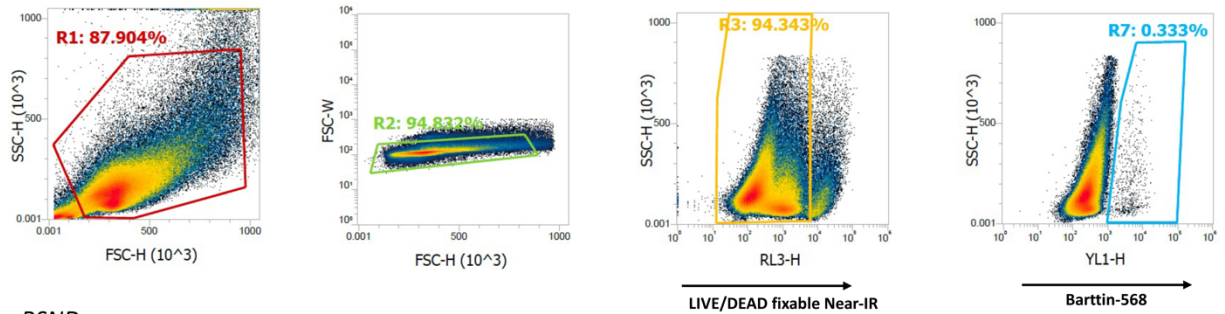


1 **Supplemental Figure 2 NKCC1 does not influence liquid absorption rates.** (A) Confocal
 2 images of human airway epithelia. The image shows barttin (white), NKCC1 (red), and nuclei
 3 (blue); scale bars = 10 μm . (B) Epithelia were transduced with a lentiviral vector expressing
 4 either GFP or a bicistronic construct expressing FOXI1 and GFP to generate and label ionocytes
 5 (FOXI1 OE), then liquid absorption rates were obtained with 100 μM bumetanide or DMSO in
 6 the basolateral solution; $n = 6$ human donors. Graph depicts mean \pm standard deviation, and
 7 Šídák-corrected P values obtained from a repeated measure one-way ANOVA are presented
 8 within the figure.

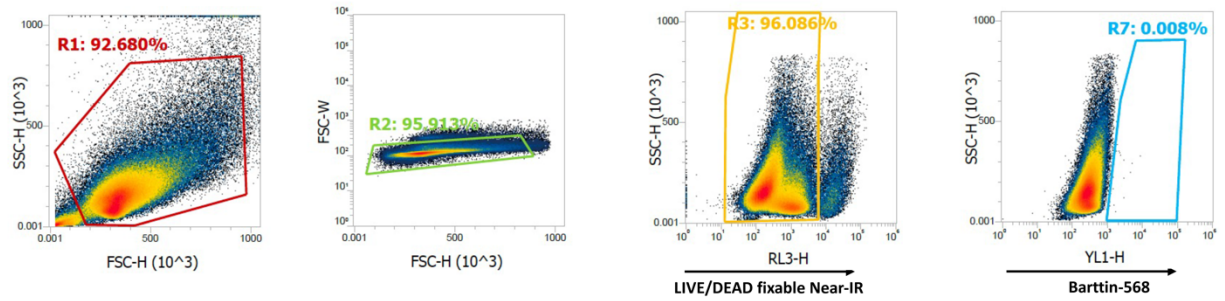
Supplemental Figure 3

A Figure 7B Example Plots

Control

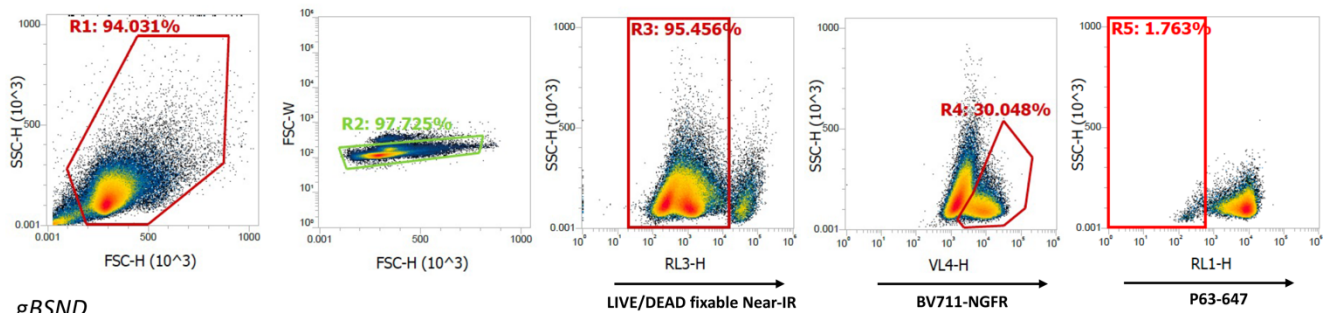


gBSND

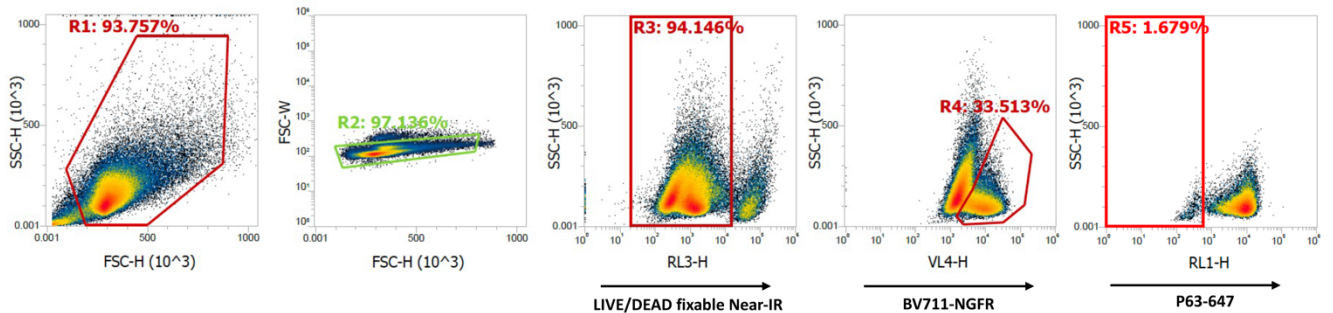


B Figure 7C Example Plots

Control



gBSND

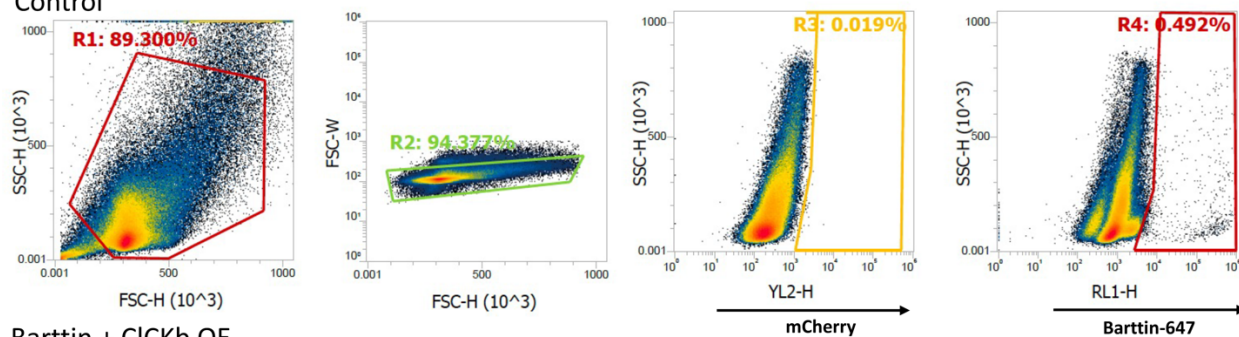


1 **Supplemental Figure 3 Example flow cytometry analysis for Figure 7, B and C.** Epithelia
2 were electroporated with CRISPR/Cas9 and guide RNAs (gRNA) targeting *BSND* (*gBSND*) to
3 decrease the amount of ionocytes that express barttin. Cells were gated by light intensities
4 detected by a flow cytometer. **(A)** Example **Figure 7B**-type experiments. The gating scheme is
5 shown from left to right. Side scatter height (SSC-H) vs. forward scatter height (FSC-H) was
6 used to select for large and granular cells. FSC-width (FSC-W) vs. FSC-H was used to exclude
7 cellular debris and clumping. Then, cells were gated for intact plasma membranes, then barttin.
8 **(B)** Example **Figure 7C**-type experiment. The first 3 gates are as described for panel **A**.
9 Additionally, cells were gated for NGFR (neuronal growth factor receptor) expression, which is
10 on basal cells and ionocytes, then p63 was used to separate basal cells (p63⁺) from ionocytes
11 (p63⁻).

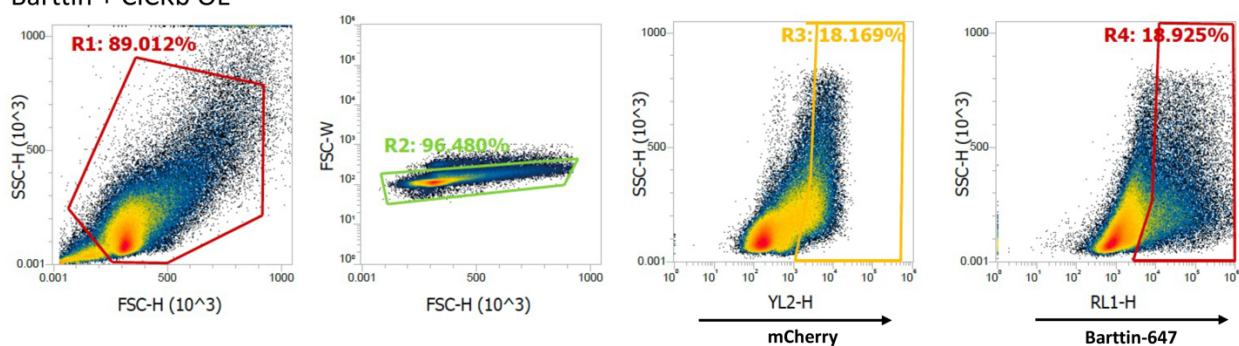
Supplemental Figure 4

A Figure 8B Example Plots

Control

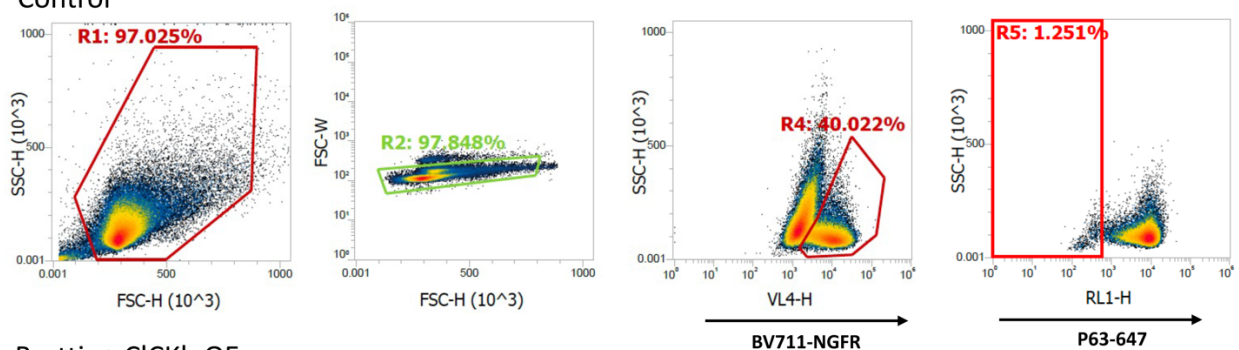


Barttin + CLICKb OE

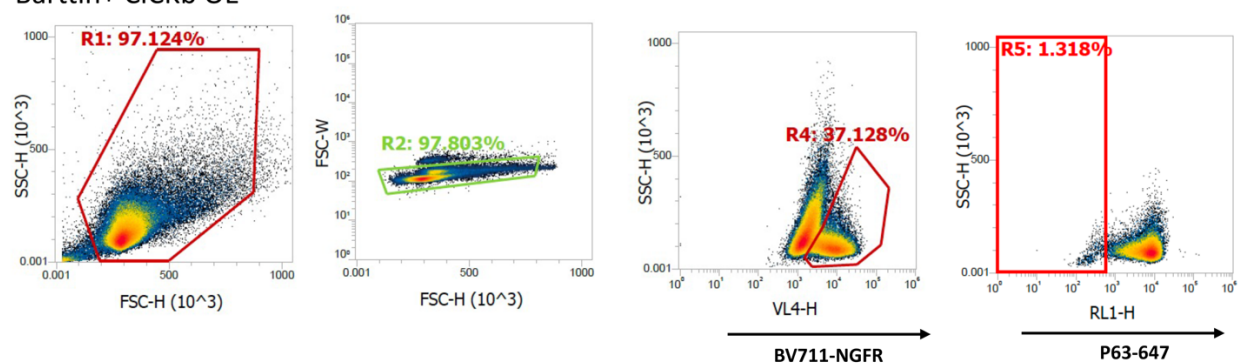


B Figure 8C Example Plots

Control

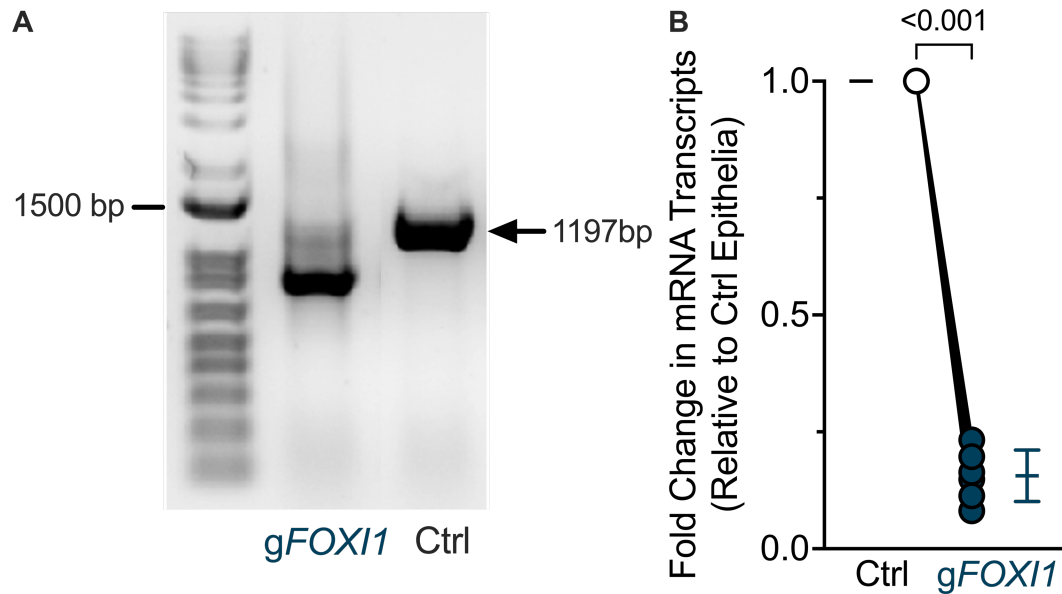


Barttin+ CLICKb OE



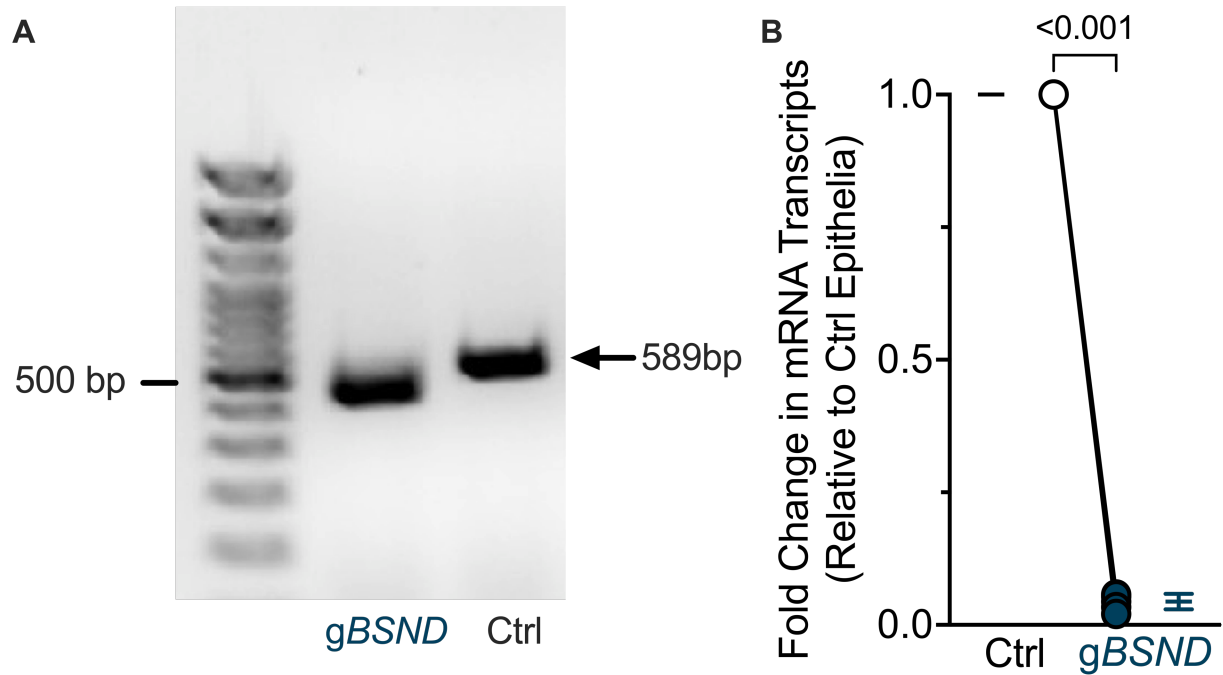
1 **Supplemental Figure 4 Example flow cytometry analysis for Figure 8, B and C.** Epithelia
2 were transduced with an adenovirus vector expressing either GFP or a vector encoding barttin,
3 ClC-Kb, and mCherry (Barttin + ClC-Kb OE) to add basolateral Cl⁻ channels to non-ionocyte
4 airway cells. Cells were gated by light intensities detected by a flow cytometer. **(A)** Example
5 **Figure 8B**-type experiments. The gating scheme is shown from left to right. Side scatter height
6 (SSC-H) vs. forward scatter height (FSC-H) was used to select for large and granular cells. FSC-
7 width (FSC-W) vs. FSC-H was used to exclude cellular debris. Within this gated population,
8 cells were sorted for mCherry (cells expressing the viral vector) or barttin. **(B)** Example **Figure**
9 **8B**-type experiment. The first 2 gates are as described for panel A. Additionally, cells were gated
10 for NGFR (neuronal growth factor receptor) expression, which is on basal cells and ionocytes,
11 then p63 was used to separate basal cells (p63⁺) from ionocytes (p63⁻).

Supplemental Figure 5



1 **Supplemental Figure 5 Controls for *FOX11* gene disruption.** (A) Genomic PCR of human
 2 airway cells electroporated with and without *gFOX11*. (B) RT-qPCR of *FOX11* transcript levels
 3 in human airway cells electroporated with and without *gFOX11*. Many *gFOX11* samples did not
 4 show amplification and a threshold cycle of 40 was used for quantification. $n = 6$ human donors.
 5 Data points connected by a line represent paired experiments from a single human donor, graph
 6 depicts mean \pm standard deviation, and the P value obtained from a paired two-sided Student's t
 7 test is presented within the figure.

Supplemental Figure 6



- 1 **Supplemental Figure 6 Controls for *BSND* gene disruption.** (A) Genomic PCR of human
- 2 airway cells electroporated with and without *gBSND*. (B) RT-qPCR of *BSND* transcript levels in
- 3 human airway cells electroporated with and without *gBSND*. Many *gBSND* samples did not show
- 4 amplification and a threshold cycle of 40 was used for quantification. $n = 6$ human donors. Data
- 5 points connected by a line represent paired experiments from a single human donor, graph
- 6 depicts mean \pm standard deviation, and the P value obtained from a paired two-sided Student's t
- 7 test is presented within the figure.
- 8